Fitoterapia 102 (2015) 182–188

Contents lists available at ScienceDirect

Fitoterapia

journal homepage: www.elsevier.com/locate/fitote

Vindogentianine, a hypoglycemic alkaloid from *Catharanthus roseus* (L.) G. Don (Apocynaceae)

Soon Huat Tiong [a], Chung Yeng Looi [b], Aditya Arya [c], Won Fen Wong [d], Hazrina Hazni [e], Mohd Rais Mustafa [b], Khalijah Awang [f,*]

[a] *Sime Darby Technology Centre, Serdang, Malaysia*
[b] *Department of Pharmacology, University of Malaya, Kuala Lumpur, Malaysia*
[c] *Department of Pharmacy, University of Malaya, Kuala Lumpur, Malaysia*
[d] *Department of Medical Microbiology, University of Malaya, Kuala Lumpur, Malaysia*
[e] *Center for Natural Product and Drug Discovery (CENAR), University of Malaya, Kuala Lumpur, Malaysia*
[f] *Department of Chemistry, University of Malaya, Kuala Lumpur, Malaysia*

ARTICLE INFO

Article history:
Received 27 November 2014
Accepted in revised form 28 January 2015
Available online 7 February 2015

Keywords:
Catharanthus roseus
Apocynaceae
Vindogentianine
Hypoglycemic
Glucose uptake
PTP-1B

ABSTRACT

Vindogentianine, a new indole alkaloid together with six known alkaloids, vindoline, vindolidine, vindolicine, vindolinine, perivine and serpentine were isolated from leaf extract (DA) of *Catharanthus roseus* (L.) G. Don. Their structures were elucidated by spectroscopic methods; NMR, MS, UV and IR. Vindogentianine is a dimer containing a vindoline moiety coupled to a gentianine moiety. After 24 h incubation, vindogentianine exhibited no cytotoxic effect in C2C12 mouse myoblast and β-TC6 mouse pancreatic cells (IC_{50} > 50 μg/mL). Real-time cell proliferation monitoring also indicated vindogentianine had little or no effect on C2C12 mouse myoblast cell growth at the highest dose tested (200 μg/mL), without inducing cell death. Vindogentianine exhibited potential hypoglycemic activity in β-TC6 and C2C12 cells by inducing higher glucose uptake and significant *in vitro* PTP-1B inhibition. However, *in vitro* α-amylase and α-glucosidase inhibition assay showed low inhibition under treatment of vindogentianine. This suggests that hypoglycemic activity of vindogentianine may be due to the enhancement of glucose uptake and PTP-1B inhibition, implying its therapeutic potential against type 2 diabetes.

1. Introduction

Catharanthus roseus (L.) G. Don (Apocynaceae) is a medicinal plant used in many traditional practices for the treatment of diabetes in several countries such as Malaysia [1], India, China, South Africa and Mexico [2]. The study of oral hypoglycemic activity led to the discovery of vinblastine and vincristine, the first natural anticancer agents used clinically [3]. This drive the attention on this plant towards anticancer and neglecting the antidiabetes activity from this plant, discovery of more than 130 alkaloids [4]. Even though with the extensive alkaloids constituent evaluation conducted onto this plant, still new indole alkaloids were discovered and reported recently. [5–8].

Therefore, several studies have reported the *in vitro* and *in vivo* activity supporting the antidiabetic activity of this plant. The extract of *C. roseus* from twig and leaves showed increase glucose utilization in cells, reduced blood glucose in animal model such as rabbits and rats [9,10]. A significant increase of glucokinase activity in the liver of rats treated with extract of this plant was also reported [11]. Some chemical constituents

Abbreviations: RTCA, real-time cell proliferation assay; TE, trolox equivalent; 2-NBDG, 2-[N-(7-nitrobenz-2-oxa-1,3-diaxol-4-yl)amino]-2-deoxyglucose; DMEM, Dulbecco's Modified Eagle Medium; FBS, fetal bovine serum; PBS, phosphate-buffered saline.

* Corresponding author at: Department of Chemistry, Faculty of Science, University of Malaya, 50603 Kuala Lumpur, Malaysia. Tel.: +60 37967 4064; fax: +60 37967 419.
E-mail address: khalijah@um.edu.my (K. Awang).

http://dx.doi.org/10.1016/j.fitote.2015.01.019
0367-326X/

of this plant had been showed to exhibit hypoglycemic activity such as vindoline, tetrahydroalstonine, catharanthine, lochericine, leurosine, vindolinine, adenosine, β-sitosterol, quercetin, ursolic acid and tannic [12–14].

However, there are still many other chemical constituents of this plant especially alkaloids, that have never been evaluated for their hypoglecemic activity. Recently, the hypoglycemic activity of several known indole alkaloids from *C. roseus* has been reported, with vindolicine (Fig. 1) showing potential as a novel protein-tyrosine phosphatase 1B (PTP-1B) inhibitor that may serve as an "insulin sensitizer" in the management of type 2 diabetes [15].

In this communication, a dimer containing a vindoline substructure coupled with a gentianine moiety, vindogentianine (**1**) was isolated from *Catharanthus roseus* (Fig. 1). This paper communicates the isolation and structure elucidation of **1**. We evaluated the *in vitro* hypoglycemic ability of **1** by glucose uptake assay, PTP-1B and α-amylase inhibition. In addition, cytotoxicity testing and antioxidant of **1** was also evaluated.

2. Results and discussion

Vindogentianine, **1** was obtained as a yellowish brown amorphous solid and was positive to Dragendoff's reagent with purity of about 90% (Fig. 1). **1** was purified from the alkaloid crude (DA) obtained from the dichloromethane (DE) leave extract of *Catharanthus roseus*. DE also showed hypoglycemic activity by exhibiting higher glucose uptake in β-TC6, mouse pancreatic cell, as compared to untreated cells [15]. Chemical investigation on the active extract led to the isolation of **1**.

The molecular formula of **1** was determined as $C_{35}H_{41}N_3O_8$ based on ESI-IT-TOFMS [*m/z* 632.3060 ($M + H^+$), Δ + 8.9 mmu] and [*m/z* 676.2897 ($M + HCOO^-$), Δ + 2.7 mmu]. IR absorptions implied the presence of hydroxyl (3458 cm^{-1}) and ester carbonyl (1741 cm^{-1}) functionalities. UV spectral absorbance's of λ_{max} (log ε): 216 (4.46), 259 (4.11) and 310 (4.01) nm suggested the presence of a dihydroindole moiety [16].

The ^{13}C NMR spectrum showed the presence of 35 carbons; four sp^3 methine, six sp^3 methylene, six methyl, six sp^2 methine and thirteen quaternary carbons. Based on comparisons of ^{13}C and ^1H NMR spectra to other earlier reported alkaloids from this plant, **1** consisted of two subunits; A and B, in which subunit A is the vindoline while subunit B is gentianine-related moeity (Fig. 1). Both units are connected through a C-10 and C-9′ linkage (Fig. 2).

The subunit A has 25 carbons consisting of three sp^3 methines, four sp^3 methylenes, five methyls, four sp^2 methines and nine quaternary that were observed in ^{13}C and DEPT 135° NMR spectra. The ^1H NMR spectrum indicated the presence of two *cis*-olefinic protons, H-14(δ_H 5.84, dd, 1H, J = 4.6, 10.1 Hz) and H-15(δ_H 5.20, d, 1H, J = 10.1 Hz). Two methoxyls attached to C-22 and C-11 resonated as two 3H singlets at δ_H 3.74 and δ_H 3.72 respectively. The presence of an acetate functionality was confirmed by the resonance of the carbonyl carbon at δ_C171.0 with the corresponding methyl carbon resonating at δ_C21.2. Two aromatic protons H-9 and H-12, appeared as singlets at δ_H 6.57 and δ_H 6.00 respectively, indicating that C-10 and C-11 were substituted. The methyl of an ethyl moiety attached to C-20 resonated as a triplet at δ_H 0.49. All the carbons and protons of the subunit A were assigned through extensive analysis of HMBC, HMQC and COSY spectra (Table 1 & Fig. 2). All chemical shifts were consistent with the reported values for vindoline.

The 10 remaining carbons were assigned to subunit B; one sp^3 methine, two sp^3 methylenes, one methyl, two sp^2 methine and four quaternary carbons. Subunit B has six degrees of unsaturation, consistent with the presence of a six membered lactone fused with a pyridine ring to give the gentianine-related moiety [11]. Two highly deshielded aromatic protons were observed as 1H singlet at δ_H 9.06 (H-3′) and δ_H 8.58 (H-

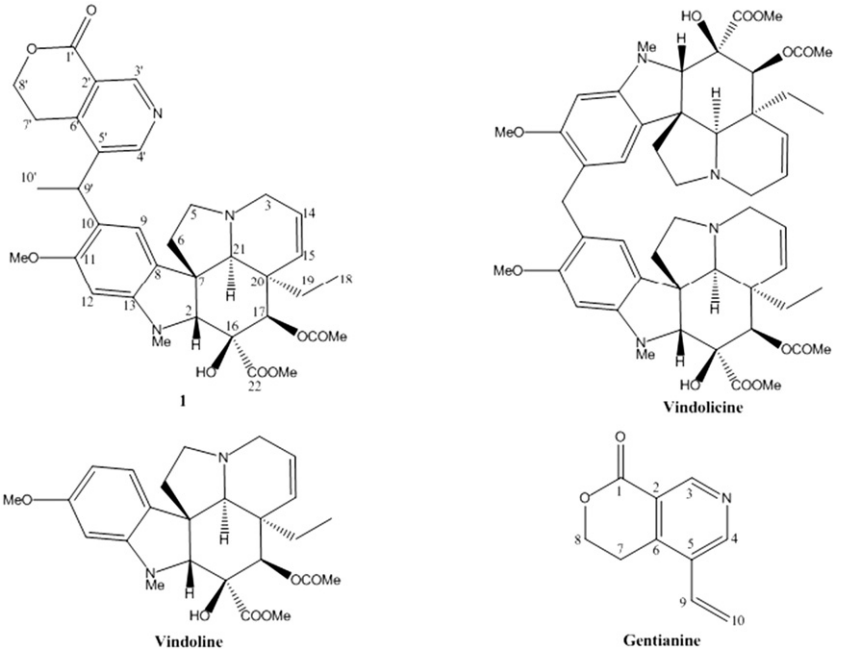

Fig. 1. Chemical structure of **1**, vindolicine, vindoline and gentianine.

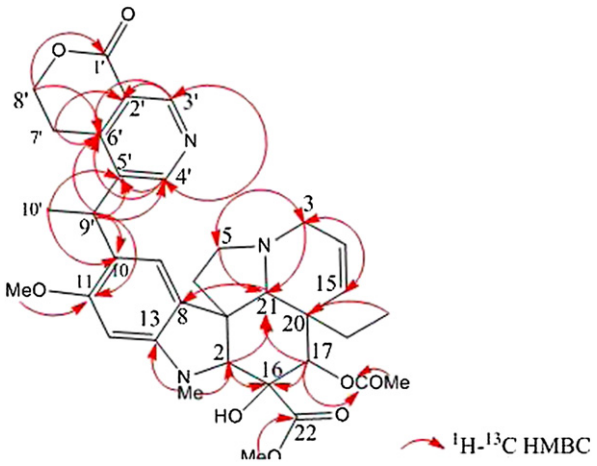

Fig. 2. Selected ^{1}H–^{13}C HMBC correlation of **1**.

4′), with corresponding carbon signals at δ_C 149.5 (C-3′) and δ_C 152.2 (C-4′), thus confirming the presence of pyridine system [11]. In addition, an overlapped signal of oxymethylene and methine signals was overlapped at δ_H 4.48 (H-8′ & H-9′). Methylene (δ_H 2.93, H-7′) and methyl (δ_H 1.48, H-10′) protons also were observed. Furthermore, ^{13}C NMR spectrum showed the C-1′ carbonyl signal at δ_C 164.3 with the corresponding ethylenyl resonance at δ_C 66.6 (C-8′) and δ_C 23.9 (C-7′).

The COSY and HMQC spectra revealed connectivity of 2 partial structures; $-OCH_2CH_2-$ and $-CHCH_3$. The former is a part of a lactone ring system while the latter is attached to the pyridine unit through C-5′. The ^{1}H–^{13}C connections between H-7′/C-2′, H-8′/C-1′, H-8′/C-6′ and H-9′/C-5′ were proven by HMBC correlation. Both the subunits A and B were connected through C-9′ and C-10 linkages. This was proven by the HMBC correlations of H-10′ to C-10 and H-9′ to C-11 (Fig. 2). C9′ was found to be a stereocentre for compound **1** but the stereochemistry of it at that position is not determined due to possible free rotation.

Gentianine is ubiquitous in Gentianaceae plants [17,18] and several genera of Apocynaceae plants such as *Alstonia* and *Hunteria* [19–21] but it has never been reported in the genus *Catharanthus*. It is believed that gentianine is an artefact formed from the degradation of gentiopicroside, a secoiridoid glycoside [22,23] also commonly found in Gentianaceae species especially in the genera *Gentiana* and *Swertia* [24,25]. We propose that **1** is a product from the coupling of the natural gentiopicroside [17] with vindoline, possibly by an enzymatic carbon-to-carbon coupling, similar to the enzymatic peroxidase coupling of vindoline and catharanthine to form vinblastine as reported [26]. Then, upon treatment with ammonia **1** was produced.

Gentianine and monoterpene indole alkaloids had been found to couple together in gentiacraline but coupling through C10–C9′ bonding such as in compound **1** has never been reported [27]. Hence, compound **1** is the first evidence for the occurrence of such coupling of gentianine related compound with monoterpene indole alkaloids.

The cytotoxicity of **1** against C2C12 mouse myoblast (skeletal muscle) and β-TC6 mouse pancreatic cell line was evaluated using MTT cell viability assay after 24 h treatment. The IC_{50} of **1** in C2C12 and β-TC6 was >50 μg/mL, whereas the cytotoxic drugs, doxorubicin exhibited IC_{50} values of 4.61 ± 0.25 μg/mL and 4.07 ± 0.19 μg/mL, and paclitaxel IC_{50} values of 3.18 ± 0.23 μg/mL and 2.85 ± 0.31 μg/mL in C2C12 and β-TC6 cells, respectively. These results clearly indicated that **1** is relatively less toxic towards C2C12 and β-TC6 cells compared to the chemotherapeutic drugs, doxorubicin and paclitaxel.

Real-time cell proliferation assay (RTCA) was carried out to monitor subtle changes in the growth pattern of C2C12 cells treated with **1** or reference cytotoxic drugs (doxorubicin or paclitaxel). The results indicated no significant difference in the proliferation of the control C2C12 cells and the cells treated with various dosages of **1** throughout the 24 hour treatment time (Fig. S1). In contrast, significant cell death was observable in samples treated with 10 μg/mL doxorubicin or paclitaxel. These results showed that **1** has little inhibitory effect towards C2C12 cell growth, consistent with our MTT cell viability results. In contrast, doxorubicin and paclitaxel inhibited cell proliferation within 6 h, implying that these drugs have a faster kinetic and higher cytotoxicity effect.

ORAC assay was conducted in order to examine whether **1** possessed antioxidant effects. This assay uses peroxyl radical as pro-oxidant and the free radical scavenging ability of the compound tested can be determined *via* Area Under Curve (AUC) calculation [28]. In this experiment, quercetin was used as the positive control for comparison of antioxidant activity. The assay performed shows that **1** exhibited relatively lower antioxidant capacity compared to the standard quercetin (Table 2).

To examine whether compound **1** can affect glucose uptake in β-TC6 pancreatic and C2C12 muscle cells, the uptake of the fluorescent hexose, 2-[N-(7-nitrobenz-2-oxa-1,3-diaxol-4-yl)amino]-2-deoxyglucose (2-NBDG), was assayed on β-TC6 and C2C12 cells. Insulin was used as positive control. The green fluorescent 2-NBDG glucose could be visualized markedly around the cytosols in **1**-treated β-TC6 and C2C12 cells (Fig. S2A). Compound **1** showed significant hypoglycemic activity at higher treatment concentrations (25.0, 50.0 & 100.0 μg/mL) as compared to untreated β-TC6 and C2C12 cells (Fig. S2B). The variable fluorescence intensities in β-TC6 and C2C12 cells treated with **1** indicated their heterogeneous glucose uptake activity.

α-Amylase is a protein enzyme that hydrolyses alpha bonds of large, alpha-linked polysaccharides, such as starch and glycogen, yielding glucose and maltose. It is the major form of amylase found in humans and other mammals [29]. Starch and disaccharides are hydrolysed by α-glucosidase in the intestine. α-Amylase and α-glucosidase are the factories for the production of glucose in blood stream from carbohydrate digestion. Protein–tyrosine phosphatase 1B (PTP-1B) is a non-receptor phospho–tyrosine protein phosphatase that negatively regulates insulin signaling by dephosphorylating the phosphotryosine residues of insulin receptors [30].

In this study, we tested the inhibitory activity of **1** against α-amylase, α-glucosidase and PTP-1B. Compounds can be considered as having a significant inhibition effect if the IC_{50} is below 50 μg/mL. The results indicated non-significant inhibition of α-amylase by **1** (74.43 ± 9.38 μg/mL) compared to acarbose (28.35 ± 3.64 μg/mL), the standard compound for α-amylase (Table 3). An effective strategy for type 2 diabetes management is the strong inhibition of α-glucosidase. This result is in relation to previous reports showing that an instant rise in the level of

Table 1
^{1}H (400 MHz) and ^{13}C (100 MHz) NMR Data of **1** compared obtained in $CDCl_3$ with ^{1}H literature of vindoline and gentianine. [41,42].

Position	1		Vindoline	Gentianine
	δ_H	δ_C	δ_H	δ_H
2	3.68 (s, 1H)	83.4	3.75	–
3	3.44 (α, dd, $1H_a$, J = 4.6, 16.3 Hz) 2.83 (β, d, $1H_b$, J = 16.3 Hz)	51.0	3.40	–
5	3.36 (α, ddd, $1H_a$, J = 4.3, 9.2, 13.7 Hz) 2.49 (β, dd, $1H_b$, J = 7.1, 10.6 Hz)	51.4	2.1–3.0	–
6	2.21 (ddd, 1H, J = 2.3, 6.8, 13.9 Hz) 2.01 (m, 1H, overlap with H_{COMe})	44.2		–
7	–	53.2	–	–
8	–	124.1	–	–
9	6.57 (s, 1H)	120.6	6.91	–
10	–	122.8	6.30	–
11	–	157.6	–	–
12	6.00 (s, 1H)	93.4	6.08	–
13	–	152.4	–	–
14	5.84 (dd, 1H, J = 4.6, 10.1 Hz)	124.6	5.88	–
15	5.20 (d, 1H, J = 10.1 Hz)	130.4	5.23	–
16	–	79.8	–	–
17	5.34 (α, s, $1H_a$)	76.5	5.43	–
18	0.49 (t, 3H, J = 7.3 Hz)	7.8	0.48	–
19	1.56 (α, m, $1H_a$, J = 7.3 Hz) 1.01 (β, m, $1H_b$, J = 7.3 Hz)	30.8	1.35	–
20	–	42.9	–	–
21	2.64 (s, 1H)	66.4	2.65	–
22	–	171.9	–	–
CO*Me*	2.03 (s, 3H)	21.2	2.07	–
NMe	2.65 (s, 3H)	38.7	2.68	–
11-OMe	3.74 (s, 3H)	55.7	3.80	–
22-OMe	3.72 (s, 3H)	52.4	3.80	–
*OCO*Me	–	171.0	–	–
1′	–	164.3	–	–
2′	–	138.6	–	–
3′	9.06 (s, 1H)	149.4	–	9.06
4′	8.58 (s, 1H)	152.2	–	8.84
5′	–	121.1	–	–
6′	–	146.5	–	–
7′	2.92 (m, 2H, overlapped with H_3)	23.9	–	3.00
8′	4.48 (m, 2H, overlapped with $H_{9'}$)	66.6	–	4.54
9′	4.48 (m, 1H, overlapped with $H_{8'}$)	31.7	–	5.77, 5.98 and 7.08
10′	1.48 (d, 3H, J = 7.3 Hz)	21.0	–	

blood glucose provokes hyperglycemia in the patients who have type 2 diabetes which might be due to hydrolysis of glucose by intestinal α-glucosidase [31]. α-Glucosidase results showed that compound **1** has an IC_{50} of 269.72 ± 15.44 μg/mL as compared to standard drug Acarbose: 165.35 ± 8.52 μg/mL (Table 3). On the other hand, low PTP-1B inhibition IC_{50} values observed for **1** (15.28 ± 2.59 μg/mL) indicated its potential effects for PTP-1B inhibition compared to RK-682 and ursolic acid, the standard control references (Table 3).

3. Conclusions

Since compound 1 showed insignificant or low digestion of carbohydrate to glucose, the glucose reduction observed in 2-NBDG glucose uptake assay was not due to reduction of glucose production. Based on these results, we proposed that compound **1** could induce higher glucose uptake in β-TC6 by lowering PTP-1B activity. Few studies have demonstrated that PTP-1B deficient mice are more sensitive to insulin, have improved glycemic control, and are resistant to diet induced obesity [31,32]. Since compound **1** showed promising inhibition of PTP-1B enzymes, therefore, it could be helpful in the management of obesity and type 2 diabetic conditions. However, the anti-diabetic effect of

Table 2
Antioxidant capacity of compounds, **1** or quercetin as determined by ORAC method.

Compound	μM TE per 100 μg/mL (±SD)
Vindogentianine	1.59 (±0.07)
Quercetin	21.41 (±0.68)

Table 3
Inhibition of α-amylase, α-glucosidase and PTP-1B by **1** compared to the standard drugs in terms of IC_{50} (dosage that inhibits 50% of enzyme activity) values.

Inhibited enzymes	Compound	IC_{50} (μg/mL)
α-Amylase	Vindogentianine	74.43 ± 9.38
	Acarbose	28.35 ± 3.64
α-Glucosidase	Vindogentianine	269.72 ± 15.44
	Acarbose	165.35 ± 8.52
PTP-1B	Vindogentianine	15.28 ± 2.59
	RK-682	5.17 ± 1.22
	Ursolic acid	4.73 ± 0.84

compound **1** warrants further in-depth molecular studies to elucidate the exact mechanism.

4. Materials and methods

4.1. General

Column chromatography: silica gel (0.063–0.200, 0.040–0.063, 0.015–0.040 mm; Merck). Preparative thin layered chromatography (PTLC): silica gel F_{254} (1 mm; Merck). UV spectra were obtained on a Shidmazu UV-1650 PC UV–vis spectrophotometer (Shimadzu); IR spectra were obtained on a Perkin-Elmer RX1 FT-IR spectrophotometer using KBr pellets, MS was recorded on a Shimadzu LCMS-IT-TOF mass spectrometer (Shidmazu); and NMR spectra were recorded on a JOEL ECA 400 FT-NMR (400 MHz/100 MHz; JOEL Delta) or Bruker Ultrashield 600 Plus (600 MHz/150 MHz; Bruker Biospin AG) spectrometer with chemical shifts in δ relative to TMS as internal reference. Dragendoff's reagent was used as the chromogenic agent. Fluorescein sodium salt, AAPH (2,2′-Azobis(2-methylpropionamidine) dihydrochloride, 97%), quercetin dehydrate (≤100%) and trolox ((±)-6-Hydroxy-2,5,7,8-tetramethylchromane-2-carboxylic acid, 97%), doxorubicin (98%), paclitaxel (>95%), ursolic acid (>90%), acarbose (>95%), RK-682 (>98%) and insulin were purchased from Sigma-Aldrich.

4.2. Plant material

C. roseus (L.) G. Don. (Apocynaceae) was cultivated at Jeli, Kelantan, Malaysia from November 2008 under natural condition. The leaves were collected in May 2009 and dried at 40 °C. The specimen was authenticated by Mr. Teo Leong Eng, a botanist in the Faculty of Science, University of Malaya. A voucher specimen with Herbarium no. of KL 5763 was deposited at the Herbarium in Department of Chemistry, University of Malaya, Kuala Lumpur, Malaysia.

4.3. Extraction and isolation

The dried leaves of *C. roseus* (1 kg) were extracted with dichloromethane (DCM) after being defatted using n-hexane. Dried ground leaves of *C. roseus* (1 kg) were macerated twice with n-hexane (10 L) for 3 days at room temperature. After removal of n-hexane, the plant residue was first wetted with 25% ammonia for 1 h followed by soaking twice with DCM (10 L) for 3 days at room temperature. The DCM extract (DE) was obtained after filtering and dried under reduced pressure. DE (42.6 g) was subjected to acid-base extraction using 5% hydrochloric acid and 25% ammonia solution to obtain an alkaloid crude extract (4.2 g) (DA).

DA was subjected to silica column chromatography (CC, diameter: 10 cm) using step gradient elution from 100% DCM to DCM:MeOH with ratios of 95:5, 90:10, 85:15, 80:20, 75:25, 70:30, 65:35, 60:40, 55:45, and 50:50 (v/v). The CC was later flushed using a solvent mixture of DCM and MeOH with a ratio of 40:60, 20:80 (v/v) before 100% MeOH. Each solvent ratio was eluted at volumes of 1000 mL. The eluent was collected into fractions of 100 mL each. Fractions with the same thin layered chromatography (TLC) profiles were then combined. A total of 15 fractions were obtained (Fractions 1–15).

Fraction 4 was applied to preparative thin layer chromatography with a solvent mixture of n-hexane:-ethyl acetate:acetone (20:79:1, v/v/v) under ammonia vapour to 0.9% yield vindogentianine, **1** (38.6 mg) from DA.

4.4. Liquid Chromatography-Ion Trap-Time of Flight-Mass Spectrometry (LCMS-IT-TOF-MS) analysis

LC-MS identification was carried out on a Shimadzu Liquid Chromatography Mass Spectrometry-Ion Trap-Time of Flight system equipped with pump (LC-20 AD), auto sampler (SIL-20 AC), column oven (CTO-20 AC), PDA detector (SPD-M20A) and coupled to an ESI interface (Shimadzu, Kyoto, Japan). Isolated compounds (5 μL, 1 mg/mL) were injected and chromatographed on a Waters XBridge C18 2.5 mm (2.1 × 50 mm) column with the mobile phases of A (0.1% formic acid in water) and B (0.1% formic acid in MeOH). The mobile phase was performed using a gradient as follows: isocratic 10% B for 2 min, linear gradient of 10% B to 100% B over the next 25 min and isocratic at 100% B for 5 min. The system was re-equilibrated for 5 min before the next sample injection. Eluent was monitored using PDA detector at 220 nm, 254 nm, 350 nm and 450 nm. ESI-MS was performed in the range 100–2000 Da in both positive and negative modes. The temperature of the heat block and curved desolvation line (the inlet for the high vacuum region) were set to 200 °C and 250 °C, respectively. Nitrogen gas was used as nebulizer with the flow rate set at 1.5 L/min. The ESI source voltage was set at 4.5 kV for positive mode and −3.5 kV for the negative mode whereas the detector was maintained at 1.7 kV. Shimadzu's LCMS solution software was used for data analysis.

4.5. Cell culture

Mouse β-TC6 pancreatic cell line and mouse myoblast (skeletal muscle) C2C12 cell line were purchased from American Type Culture Collection (ATCC, Manassas, VA, USA). C2C12 cells were grown in Dulbecco's Modified Eagle Medium (DMEM, Life Technologies, Inc., Rockville, MD) supplemented with 10% heat-inactivated fetal bovine serum (FBS, Sigma-Aldrich, St. Louis, MO), 1% penicillin and streptomycin. β-TC6 was cultured in 15% heat-inactivated fetal bovine serum (FBS, Sigma-Aldrich, St. Louis, MO), 1% penicillin and streptomycin in Dulbecco's Modified Eagle Medium (DMEM, Life Technologies, Inc., Rockville, MD) [33]. The cultures were kept in a humidified incubator at 37 °C in 5% CO_2 and the growth medium was changed every 3 days.

4.6. Cytotoxicity assay

The cytotoxic effect of **1** was assessed by MTT cell viability assay as described previously [34]. 1.0×10^4 cells were seeded in a 96-well plate and incubated overnight at 37 °C in 5% CO_2. On the next day, the cells were treated with a two-fold dilution series of seven dosages (100, 50, 25, 12.5, 6.25, 3.125, 1.56 μg/mL) of the compound, and then they were further cultured for 24 h. MTT solution (4,5-dimethylthiazol-2-yl-2,5-diphenyltetrazoliumbromide) was added at 2 mg/mL and after 2 h of incubation at 37 °C in 5% CO_2, DMSO was added to dissolve the formazan crystals. The plates were then read in Chameleon multi technology micro plate reader (Hidex, Turku,

Finland) at 570 nm absorbance. Cell viability was calculated by previously described method [35,30]. The ratio of the absorbance of treated cells to the absorbance of DMSO-treated control cells was determined as percentage of cell viability. IC_{50} value was defined as the concentration of the compound required to reduce the absorbance of treated cells to 50% of the DMSO-treated control cells. The experiment was carried out in triplicates.

4.7. Real-time cell proliferation

In vitro proliferation of **1**-treated and untreated mouse myoblast C2C12 cells was examined using Roche xCELLigence Real-Time Cellular Analysis system (Roche, Manheim, Germany). On the first day, 1.0×10^4 cells were seeded in each well of a 16X E-plate background measurement, which was done by adding 100 mL of the appropriate medium to the wells. The real-time cellular analysis system monitored the proliferation of cells every 5 min for about 20 h. During the log growth phase, the cells were treated with different concentrations (12.5, 25, 50, 100 and 200 μg/mL) of **1** or 10 μg/mL of doxorubicin or paclitaxel and monitored continuously for another 24 h.

4.8. Oxygen Radical Antioxidant Capacity (ORAC)

ORAC assay was done with slight modifications to previously reported methods [36]. Compound **1** was diluted to a final concentration of 100 μg/mL, with total reaction volume of 200 μL. The assay was performed in a 96-well black micro plate, with 25 μL of **1**, standard (trolox), blank (solvent) or positive control (quercetin). Subsequently, 150 μL of working fluorescein solution was added to each well of assay plate. The plate was incubated at 37 °C for 15 min. 25 μL of AAPH working solution was then added to the wells, making up a total volume of 200 μL. Fluorescence was recorded with excitation wavelength of 485 nm and emission wavelength of 538 nm. Data were collected for duration of 2 h, and were analysed by calculating the differences of area under fluorescence decay curve of samples and blank. The values were expressed as Trolox Equivalent (TE).

4.9. 2-NBDG glucose uptake

β-TC6 or C2C12 cells were seeded at a density of 1.5×10^4 cells/mL in 96-well plate and allowed to attach, spread, and proliferate to near confluence at 37 °C in 5% CO_2. After an overnight incubation, the medium was discarded, washed with phosphate-buffered saline (PBS) twice and replenished with 2.5 mM glucose in basal medium comprising DMEM without glucose or pyruvate supplemented with L-glutamine and 15% (v/v) FBS (final serum glucose concentration of approximately 0.25 mM).

The cells were incubated for 60 min at 37 °C in 5% CO_2. The conditioning medium was then replaced with 10 mM 2-NBDG (Invitrogen) in basal medium in the presence or absence of **1**. The cells were kept at 37 °C in 5% CO_2 for 30 min to permit endocytosis of the 2-NBDG. Then, the medium was removed, cells were washed twice with PBS and stained with nucleic dye Hoechst 33342 for another 30 min. The cells were then observed for intra-cellular fluorescence at Excitation/Emission = 350 nm/461 nm and Excitation/Emission = 475 nm/550 nm for Hoechst 33342 and 2-NBDG, respectively. Plates were evaluated using the Array Scan High Content Screening system (Cellomics Inc., Pittsburgh, PA, USA) and analysed with Target Activation BioApplication software (Cellomics Inc.) [37].

4.10. α-Amylase inhibition assay

Sample (500 μL) and 500 μL of 0.02 M sodium phosphate buffer (pH 6.9 with 0.006 M NaCl) containing α-amylase solutions (0.5 mg/mL) were incubated at 25 °C for 10 min [38]. α-Amylase from *Bacillus licheniformis* was procured from Sigma-Aldrich (USA). After pre-incubation, 500 μL of a 1% starch solution in 0.02 M sodium phosphate buffer (pH 6.9 with 0.006 M sodium chloride) was added to each tube at timed intervals. The reaction mixtures were then incubated at 25 °C for 10 min. The reaction was stopped with 1.0 mL of dinitrosalicylic acid colour reagent. The test tubes were then incubated in a boiling water bath for 5 min and cooled to room temperature. Acarbose was used as a standard positive. The reaction mixture was then diluted after adding 10 mL distilled water and absorbance was measured at 540 nm using multimode-reader. The results were expressed as % inhibition of enzyme activity.

4.11. α-Glucosidase inhibition assay

In this method, α-glucosidase from *Saccharomyces cerevisiae* was obtained from Sigma-Aldrich (USA). α-Glucosidase (20 μL, 1.5 U/mL) was premixed with 200 μL of test compounds at varying concentrations made up in 50 mM phosphate buffer at pH 6.8 and incubated for 5 min at 37 °C. 1 mM para-nitrophenyl-α-D glucopyranoside (200 μL) in 50 mM of phosphate buffer was added to initiate the reaction, and the mixture was further incubated at 37 °C for 20 min. Acarbose was used as the positive control. The reaction was terminated by the addition of 500 μL of 1 M Na_2CO_3, and the final volume was made up to 1500 μL. The absorbance was recorded at 405 nm [39].

4.12. PTP-1B inhibition assay

The present study investigated **1** for its inhibitory effects on protein–tyrosine phosphatase 1B (PTP-1B) activity in an *in vitro* assay. Ursolic acid and 3-hexadecanoyl-5-hydroxymethyl tetronic acid (RK-682) were used as positive controls in the assay [40]. To each well of a 96-well plate (final volume: 200 μL), 2 mM p-nitrophenyl phosphate (p-NPP) as a substrate and PTP-1B human recombinant enzyme (BIOMOL International LP USA) (0.1 μg) were added in a 50 mM citrate buffer of pH 6.0, containing, 0.1 M NaCl, 1 mM EDTA, and 1 mM dithiothreitol (DTT) with or without fraction samples and incubated for 30 min at 37 °C. Thereafter, 10 M NaOH was added and the reaction was terminated. The amount of *p*-nitro phenol produced was estimated by measuring the absorbance at 405 nm. The non-enzymatic hydrolysis of 2 mM p-NPP was measured at the same absorbance in the absence of PTP-1B enzyme.

4.13. Statistical analysis

Data were presented as means ± SEM (standard error of mean) and analysed with unpaired Student's *t*-test. $p < 0.05$ is considered significant.

4.14. Vindogentianine (1)

Yellowish brown amorphous; mp 132–138 °C; UV (MeOH) λ_{max} (log ε) 216 (4.46), 259 (4.11) and 310 (4.01) nm; $[\propto]_D^{22}$ – 134 (*c*0.01, MeOH); IR (KBr) ν_{max} 3458, 1741 and 1240 cm^{-1}; ^1H and ^{13}C NMR ($CDCl_3$, 400 and 100 MHz, Table 1); ESI MS (+ve) *m/z* 632.3 [M + H]+; ESI MS (−ve) *m/z* 676.3 [M + HCOO]-; ESI-IT-TOF-MS *m/z* 632.3060 [M + H] + (calcd for $C_{35}H_{41}N_3O_8$ *m/z* 631.2894).

Conflict of interest

The authors declare no conflict of interest.

Acknowledgements

This work was supported by Post Graduate Research Fund (PS368/2010B), UM research fund (RG041-10BIO) and High Impact Research grant (HIR: E00002-20001) from University of Malaya.

Appendix A. Supplementary data

Supplementary data to this article can be found online at http://dx.doi.org/10.1016/j.fitote.2015.01.019.

References

[1] Ong HC, Ahmad N, Milow P. Traditional medicinal plants used by the temuan villagers in Kampung Tering, Negeri Sembilan, Malaysia. Ethnop Med 2011;5:169–73.
[2] Patel DK, Kumar R, Laloo D, Hemalatha S, et al. Natural medicines from plant source used for therapy of diabetes mellitus: an overview of its pharmacological aspects. Asian Pac J Trop Dis 2012;2(3):239–50.
[3] Sottomayor M, Ros Barcelo A. The vinca alkaloids: from biosynthesis and accumulation in plant cells, to uptake, activity and metabolism in animal cells. In: Atta-ur R, editor. Studies in natural products chemistry (Bioactive natural products). Amsterdam: Elsevier Science Publisher; 2005. p. 813–57.
[4] Blasko G, Cordell GA. Isolation structure elucidation and biosynthesis of bisindole alkaloids of Catharanthus. In: Cordell GA, editor. The alkaloids. San Diego: Academic Press; 1990. p. 1–76.
[5] Zhang W-K, et al. Two new vinblastine-type N-oxide alkaloids from *Catharanthus roseus*. Nat Prod Res 2013;27(20):1911–6.
[6] Wang C-H, et al. Cytotoxic dimeric indole alkaloids from *Catharanthus roseus*. Fitoterapia 2012;83(4):765–9.
[7] Wang CH, Wang GC, Wang Y, Zhang XQ, Huang XJ, Ye WC, et al. Three new monomeric indole alkaloids from the roots of *Catharanthus roseus*. J Asian Nat Prod Res 2012;14(3):249–55.
[8] Wang L, He HP, Di YT, Zhang Y, Hao XJ, et al. Catharoseumine, a new monoterpenoid indole alkaloid possessing a peroxy bridge from *Catharanthus roseus*. Tetrahedron Lett 2012;53(13):1576–8.
[9] Singh SN, et al. Effect of an antidiabetic extract of *Catharanthus roseus* on enzymic activities in streptozotocin induced diabetic rats. J Ethnopharmacol 2001;76(3):269–77.
[10] Nammi S, Boini MK, Lodagala SD, Behara RBS, et al. The juice of fresh leaves of *Catharanthus roseus* Linn. reduces blood glucose in normal and alloxan diabetic rabbits. BMC Complement Altern Med 2003;3(1):4.
[11] van de Venter M, et al. Antidiabetic screening and scoring of 11 plants traditionally used in South Africa. J Ethnopharmacol 2008;119(1):81–6.
[12] Marles R, Farnsworth N. Antidiabetic plants and their active constituents. Phytomedicine 1995;2(2):137–89.
[13] Raju MG, Satyanarayana S, Kumar KE. Safety of Gliclazide with the aqueous extract of Vinca rosea on pharmacodynamic activity in normal and alloxan induced diabetic rats. J Pharm Res 2012;5(3).
[14] Svoboda GA. The alkaloids of *Catharanthus roseus* G. Donn (Vinca rosea L.) in cancer chemotheraphy. In: Gunkel JE, editor. Current topics in plant science. New York: Academic Press; 1969. p. 303–35.
[15] Tiong SH, et al. Antidiabetic and antioxidant properties of alkaloids from *Catharanthus roseus* (L.) G. Don. Molecules 2013;18(8):9770–84.
[16] Gorman M, Neuss N, Svoboda GH, Barnes AJ, Cone NJ, et al. A note on the alkaloids of Vinca rosea Linn. (*Catharanthus roseus* G. Don.) II. Catharanthine, lochnericine, vindolinine, and vindoline. J Am Pharm Assoc 1959;48(4):256–7.
[17] Wang D, Xu M, Zhu HT, Chen KK, Zhang YJ, Yang CR, et al. Biotransformation of gentiopicroside by asexual mycelia of Cordyceps sinensis. Bioorg Med Chem Lett 2007;17(11):3195–7.
[18] Siegler DS. Plant systematics and alkaloids. In: Manske RHF, editor. The alkaloidsL chemistry and physiology. New York: Academic Press; 1977.
[19] Cherif A, Massiot G, Le Men-Olivier L, Pusset J, Labarre S, et al. Alkaloids of Alstonia coriacea. Phytochemistry 1989;28(2):667–70.
[20] Legseir B, Cherif A, Richard B, Pusset J, Labarre S, Massiot G, Le Men-Olivier L, et al. Alkaloids of Alstonia lenormandii, a structural revision of 10-methoxycompactinervine. Phytochemistry 1986;25(7):1735–8.
[21] Lavaud C, Massiot G, Vercauteren J, Le Men-Olivier L, et al. Alkaloids of Hunteria zeylanica. Phytochemistry 1982;21(2):445–7.
[22] Clivio P, et al. Alkaloids from leaves and stem bark of Ervatamia polyneura. Phytochemistry 1990;29(9):3007–11.
[23] El-Sayed A, Handy GA, Cordell GA. Catharanthus Alkaloids, XXXVIII. Confirming Structural evidence and antineoplastic activity of the bisindole alkaloids leurosine-N'b-oxide (pleurosine), roseadine, and vindolicine from *Catharanthus roseus*. J Nat Prod 1983;46(4):517–27.
[24] Wachsmuth O, Matusch R. Anhydronium bases from Rauvolfia serpentina. Phytochemistry 2002;61(6):705–9.
[25] Cordell GA. The monoterpene alkaloids. In: Manske RHF, editor. The alkaloids: chemistry and physiology. New York: Academic Press; 1977. p. 431–510.
[26] Endo T, Goodbody A, Vukovic J, Misawa M, et al. Enzymes from *Catharanthus roseus* cell suspension cultures that couple vindoline and catharanthine to form 3′, 4′-anhydrovinblastine. Phytochemistry 1988;27(7):2147–9.
[27] Guillaume D, et al. Some alkaloids of Alstonia undulata. Phytochemistry 1984;23(10):2407–8.
[28] Paydar M, Wong YL, Moharam BA, Wong WF, Looi CY, et al. In vitro anti-oxidant and anti-cancer activity of methanolic extract from Sanchezia speciosa leaves. Pak J Biol Sci 2013;16(20):1212–5.
[29] Pugh MD. Stedman's Medical Dictionary. 27th ed. Baltimore: Lippincott Williams & Wilkins; 2000.
[30] Klaman LD, et al. Increased energy expenditure, decreased adiposity, and tissue-specific insulin sensitivity in protein-tyrosine phosphatase 1B-deficient mice. Mol Cell Biol 2000;20(15):5479–89.
[31] Gray GM. Carbohydrate digestion and absorption. Role of the small intestine. N Engl J Med 1975;292(23):1225.
[32] Elchebly M, et al. Increased insulin sensitivity and obesity resistance in mice lacking the protein tyrosine phosphatase-1B gene. Science 1999; 283(5407):1544–8.
[33] Poitout V, Stout LE, Armstrong MB, Walseth TF, Sorenson RL, Robertson RP, et al. Morphological and functional characterization of βTC-6 cells—an insulin-secreting cell line derived from transgenic mice. Diabetes 1995; 44(3):306–13.
[34] Gummadi VR, et al. Discovery of 7-azaindole based anaplastic lymphoma kinase (ALK) inhibitors: wild type and mutant (L1196M) active compounds with unique binding mode. Bioorg Med Chem Lett 2013;23(17):4911–8.
[35] Looi CY, et al. Octa-arginine mediated delivery of wild-type Lnk protein inhibits TPO-induced M-MOK megakaryoblastic leukemic cell growth by promoting apoptosis. PLoS One 2011;6(8):e23640.
[36] Arya A, Cheah SC, Looi CY, Taha H, Mustafa MR, Mohd MA, et al. The methanolic fraction of Centratherum anthelminticum seed downregulates pro-inflammatory cytokines, oxidative stress, and hyperglycemia in STZ-nicotinamide-induced type 2 diabetic rats. Food Chem Toxicol 2012; 50(11):4209–20.
[37] Loaiza A, Porras OH, Barros LF. Glutamate triggers rapid glucose transport stimulation in astrocytes as evidenced by real-time confocal microscopy. J Neurosci 2003;23(19):7337–42.
[38] Apostolidis E, Kwon Y-I, Shetty K. Inhibitory potential of herb, fruit, and fungal-enriched cheese against key enzymes linked to type 2 diabetes and hypertension. Innovative Food Sci Emerg Technol 2007;8(1):46–54.
[39] Shinde J, et al. α-Glucosidase inhibitory activity of Syzygium cumini (Linn.) Skeels seed kernel in vitro and in Goto–Kakizaki (GK) rats. Carbohydr Res 2008;343(7):1278–81.
[40] Hoang DM, et al. Protein tyrosine phosphatase 1B inhibitors isolated from Morus bombycis. Bioorg Med Chem Lett 2009;19(23):6759–61.
[41] Gorman M, Neuss N, Biemann K. Vinca alkaloids. X1. The structure of vindoline. J Am Chem Soc 1962;84(6):1058–9.
[42] Wenkert E, et al. Carbon-13 nuclear magnetic resonance spectroscopy of naturally occurring substances. XIX. Aspidosperma alkaloids. J Am Chem Soc 1973;95(15):4990–5.